Optik ▮ (▮▮▮▮) ▮▮▮–▮▮▮

Contents lists available at ScienceDirect

Optik

journal homepage: www.elsevier.de/ijleo

A 2D rods-in-air square-lattice photonic crystal optical switch

H.Z. Wang [a], W.M. Zhou [b], J.P. Zheng [a,*]

[a] Department of Electrical and Computer Engineering, Florida A&M University and Florida State University, Tallahassee, FL 32310, United States
[b] Sensors and Electron Devices Directorate, US Army Research Laboratory, Adelphi, MD 20783-1197, United States

ARTICLE INFO

Article history:
Received 1 March 2009
Accepted 10 June 2009

Keywords:
Photonic crystal
Optical switches

ABSTRACT

A 2D photonic crystal optical switch is proposed based on a rods-in-air square-lattice photonic crystal by removing two cross-lines of rods from a 2D square-lattice photonic crystal to form four optical channels. The simulation results show that, when inserting a single rod along the diagonal line of the intersection area of two removed cross-lines of rods, the position of the single inserted rod determines how much incident energy goes into different channels. In the case of transverse magnetic (TM) Gaussian point source, time domain simulation shows that up to 87.3% of the incident energy can be switched into a channel, which is vertical to the source channel. Because there are two diagonal lines in the intersection area of two removed cross-lines of rods, the optical switch feature is achieved by shifting the inserted rod between two diagonal lines. It is also found that the magnitude of the reflected wave in the source channel varies greatly with spatial position of the single inserted rod. The larger the magnitude of the reflected wave in the source channel, the less the energy that goes into the switched channel. The time delay between the incident wave and the reflected wave in the source channel is also related to the position of the single inserted rod. In addition, the large time delay between the incident wave and the reflected wave in the source channel shows that the reflected wave encounters many reflections with the walls of the source channel, instead of waves reflected back from the single inserted rod.

1. Introduction

The photonic crystal (PhC) concept was proposed in 1987 [1,2], and the first 3D experimental photonic crystal with full band gap was manufactured in 1991. The remarkable property of PhC is the existence of the band gap in the PhC bulk. The modes in the band gap could not propagate through the bulk of PhC. The existence of a band gap, which classical optical materials do not have, results from the periodic structure of PhC. Due to the existence of this band gap, PhC has special properties such as cavity, superprism, negative refraction, nonlinear property, and magneto-optical Faraday effect. Consequently it provides many new potential applications such as fiber, waveguide, add-drop multiplexer, superprism, switch, and heterostructures device.

The PhC switch function is realized by changing the index of PhC by heating [3,4], changing conductance of semiconductor in the PhC structure [5], changing design parameters of the PhC structure [6], inserting different PhC structures into optical network with microelectromechanical (MEMS) technology [7–10], changing the incident angle [11], and changing Kerr coefficient in the PhC cavity [12–16]. A 2D rods-in-air square-lattice photonic crystal optical switch is proposed and discussed in this paper. It is constructed by removing two cross-lines of rods from a 2D square-lattice photonic crystal and then inserting a single rod along the diagonal line of the intersection area, which is formed by two removed cross-lines rods. The optical switch feature is realized by shifting the position of the single inserted rod between the two diagonal lines. When the TM Gaussian mode propagates from the left channel, the incident energy is distributed to different channels with the change in the position of the single inserted rod. The incident energy going into the upper channel is greater than that going into the right and the down channels when the position of single inserted rod is on one diagonal line of the intersection area. Because of the 2D rods-in-air square-lattice PhC switch is a symmetric structure, where there are two diagonal lines in the intersection area. When the single inserted rod shifts to another diagonal line in the intersection area, the incident energy going into the down channel is much more than that going into the right and upper channels. Through jumping of a single inserted rod between two diagonal lines in the intersection area, the incident energy is switched to the upper or down channel.

A practical method to fabricate this 2D rods-in-air square-lattice photonic crystal optical switch is MEMS technology [8,17]. This 2D rods-in-air square-lattice photonic crystal structure and

* Corresponding author. Fax: +1 850 4106479.
E-mail address: zheng@eng.fsu.edu (J.P. Zheng).

0030-4026/$ - see front matter © 2009 Elsevier GmbH. All rights reserved.
doi:10.1016/j.ijleo.2009.06.002

Report Documentation Page

Form Approved
OMB No. 0704-0188

1. REPORT DATE	2. REPORT TYPE	3. DATES COVERED
MAR 2009		**00-00-2009 to 00-00-2009**

4. TITLE AND SUBTITLE	5a. CONTRACT NUMBER
A 2D rods-in-air square-lattice photonic crystal optical switch	5b. GRANT NUMBER
	5c. PROGRAM ELEMENT NUMBER
6. AUTHOR(S)	5d. PROJECT NUMBER
	5e. TASK NUMBER
	5f. WORK UNIT NUMBER
7. PERFORMING ORGANIZATION NAME(S) AND ADDRESS(ES) **US Army Research Laboratory,Sensors and Electron Devices Directorate,Adelphi,MD,20783-1197**	8. PERFORMING ORGANIZATION REPORT NUMBER
9. SPONSORING/MONITORING AGENCY NAME(S) AND ADDRESS(ES)	10. SPONSOR/MONITOR'S ACRONYM(S)
	11. SPONSOR/MONITOR'S REPORT NUMBER(S)

12. DISTRIBUTION/AVAILABILITY STATEMENT
Approved for public release; distribution unlimited

13. SUPPLEMENTARY NOTES

14. ABSTRACT
see report

15. SUBJECT TERMS

16. SECURITY CLASSIFICATION OF:			17. LIMITATION OF ABSTRACT	18. NUMBER OF PAGES	19a. NAME OF RESPONSIBLE PERSON
a. REPORT **unclassified**	b. ABSTRACT **unclassified**	c. THIS PAGE **unclassified**	**Same as Report (SAR)**	**6**	

other similar structures were also investigated by simulations and experiments from other perspectives, for example, beam splitter and cross-talk [18–25]. Here, it is discussed with more details from the perspective of an optical switch application. The distribution of light among channels is the emphasis of this investigation and hence time domain simulations run two-dimensionally. Because the real optical switches are 3D devices, the loss of light out of the 2D PhC plane is the primary concern for the application of this 2D planer optical switch. One possible approach to constrain this light loss out of 2D PhC plane is to position a 2D optical switch between Bragg mirrors, cladding layers [4,26].

2. Simulation

Fig. 1 shows the top view of a 2D PhC optical switch with a rods-in-air structure. It is produced by removing two vertical and horizontal lines of rods from a square-lattice PhC. The lattice constant of PhC is a. The rod represented by the solid circles in Fig. 1 is a high-index cylinder with diameter $0.4a$. The dielectric constant ε_r of the high-index rod is 12, corresponding to silicon at a wavelength of 1500 nm. The frequency property of the 2D square-lattice PhC was simulated by the MIT Photonic-Bands (MPB) software. Its method to calculate Maxwell's equations is the block-iterative frequency-domain methods [27]. After simulation, it was found that the 1st TM band gap (Fig. 2) is from frequency $0.28c/a$ to $0.42c/a$, where the frequency unit is represented as c/a, and c is the speed of light in vacuum.

During the simulation, the coordinate is established as follows: the original point is at the center of the two removed lines as shown in Fig. 1, the x-axis is toward the left, the y-axis is down, and the z-axis is vertical to the paper and points away from the readers. The length of unit is lattice constant (a) of PhC. The time domain simulations were designed as follows: a point source was positioned in the left channel at $(-8,0)$, and emitted light uniformly in the x–y plane. It sent a TM Gaussian pulse with a center frequency of $0.35c/a$ and a pulse width of $20a/c$. TM wave means that electric field intensity E has non-zero component only in the z-axis, i.e. $E_x=0$, $E_y=0$, and $E_z\neq 0$. Since the electric field intensity E and magnetic field intensity H are always perpendicular to each other, $H_x\neq 0$, $H_y\neq 0$, and $H_z=0$. Four detectors with length $2a$ were vertically positioned at four channels. The centers of four detectors are $(-7,0)$ for left detector, $(7,0)$ for right detector, $(0,-7)$ for upper detector and $(0,7)$ for down detector. Each detector accumulates the net energy flow that flowed in the corresponding channel. Each detector is assigned a direction, which designates its direction of positive energy flow. When an energy flow passes through a detector along its direction, this energy flow is considered as positive energy flow. If an energy flow passes through a detector opposite to its direction, this energy flow is considered as negative energy flow. When reflection phenomena exist during the simulations, light passes through a detector from both sides. By the end of simulation, a detector accumulates the net energy along the detector's direction, i.e. the sum of positive energy flows minus that of the negative energy flows. The directions of the four detectors are positive direction of the x-axis for the left and right detectors, negative direction of the y-axis for the upper detector, and positive direction of the y-axis for the down detector. All detectors are transparent to light, i.e. no influence to propagation of light. An additional high-index ($\varepsilon_r=12$) single rod with same geometric property (diameter=$0.4a$) was inserted along the diagonal line segment of the intersection area of two removed cross-lines of rods. The intersection area is a square with four vertexes, $(1,1)$, $(1,-1)$, $(-1,-1)$, and $(-1,1)$. This diagonal line segment starts at $(-0.7,-0.7)$ and ends at $(0.7,0.7)$. The simulation results illustrate that the position of the single inserted rod controls the quantity of light entering the different channels. The time domain simulations were implemented by software MEEP. MEEP uses the finite-difference time-domain (FDTD) method to implement electromagnetic field computations. The entire simulation area is $20a\times 40a$. A perfectly matched layer (PML) with a thickness of one lattice constant was the inside wall for the entire simulation area. In simulations, application of PML boundary condition absorbed numerical reflections at the boundary of computational area and consequently provided an accurate solution [28]. The simulation ran 500 time unit (a/c) in order to make the light disappear by the end of the simulation.

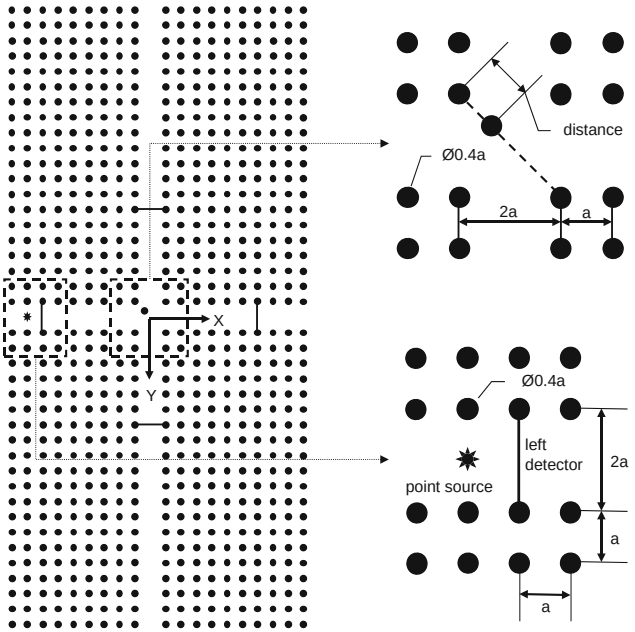

Fig. 1. Top view of 2D rods-in-air square-lattice PhC optical switch. Areas close to the source and the inserted rod are separately enlarged as two small figures on the right side. Solid circles represent high-index material (ε_r=12). The entire simulation area is $20a\times 40a$. Note that x-axis is toward the left, y-axis down, and z-axis vertical to paper pointing away from readers. The origin is located at the center of cross-area, as indicated. In the small right-up figure, the diagonal line is represented as dash line, from $(-7,-7)$ to $(7,7)$. Another diagonal line, from $(-7,7)$ to $(7,-7)$, is not depicted in this figure.

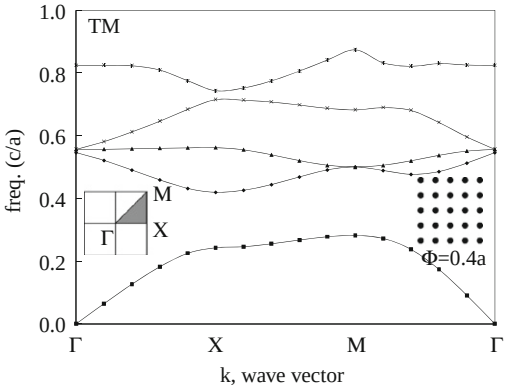

Fig. 2. TM band diagram of square lattice photonic crystals with lattice constant a. The diameter of rod is $0.4a$ and the dielectric constant of rod is $12a$. The 1st TM band gap frequency is from $0.28c/a$ to $0.42c/a$, where the frequency unit is represented as c/a, and c is the speed of light in vacuum.

Please cite this article as: H.Z. Wang, et al., A 2D rods-in-air square-lattice photonic crystal optical switch, Opt. Int. J. Light Electron. Opt. (2010), doi:10.1016/j.ijleo.2009.06.002

3. Results and discussions

Fig. 3 shows a snapshot of electric field intensity (E_z) distribution in 2D PhC optical switch at time $106a/c$. This snapshot shows that most incident energy goes into the upper channel. Even though only E_z is illustrated in Fig. 3, this snapshot also represents the energy flow. This is because the energy flow of the EM wave is expressed by the Poynting vector $p=E\times H$. Moreover, light propagation is the result of interaction between the electric and magnetic fields. Hence, electric field E and magnetic field H overlap in space and time. Energy flow was measured by the net energy flowing out of the PhC for the right, upper, and down channels, and flowing in of the PhC for the left channel. Fig. 3 also demonstrates that some light propagates inside the PhC rather than inside the channels. The energy flow that propagates inside PhC could not be counted by the detectors since the length of detectors is $2a$.

The relation between net energy flow in each channel and the position of a single inserted rod is shown in Fig. 4, where the x-axis is the position of the single inserted rod, the y-axis is the ratio of the net energy flow in channels after unification with incident energy to the left channel, which, in fact, is the positive energy flow of the left detector. In Fig. 4, the ratio of net energy flow of the upper channel follows that of the left channel. When the position of the single inserted rod is far away from the center $(0,0)$, much of the incident light along the left channel goes into the upper channel. When the single inserted rod is close to the center $(0,0)$, less of the incident light enters the upper channel. Indeed, much of the incident light from the left channel is reflected back into the left channel under such case. This similarity of the net energy flow ratio in both left channel and upper channel indicates the control effect of this 2D rods-in-air PhC structure on the incident light from the left channel. The maximum net energy flow ratio of the upper channel, 87.3%, occurs when the distance is $1.98a$ $(0.4,0.4)$. The minimum energy ratio of the upper channel is only 2.5%, corresponding to a distance of $1.41a$ $(0,0)$. It should be pointed out that the point source sent one half of the total source energy along the negative x-axis and another half of the total source energy along the positive x-axis in the left channel. The first half of the total source energy, heading into negative x-axis, is absorbed by the PML boundary condition when it impinges the boundary of simulation area. This half of the total source energy did not pass the left detector and is beyond discussion. Another half of the total source energy, which propagates along the positive x-axis, is the incident wave of the left channel. The contrast between the maximum and minimum energy flow ratios is 35.

It is also shown in Fig. 4 that the curves of the net energy flow ratio between the left channel and the upper channel are very close, with less than 5% difference of the net energy flow ratio, in the distance range of $1.8a$–$2.0a$. This demonstrates that more light from the left channel goes into the upper channel when a single rod was inserted in the distance range $1.8a$–$2.0a$. Consequently, the switching efficiency of the optical switch in the distance range $1.8a$–$2.0a$ is the highest among the entire range of distance. In the case of no single inserted rod, the ratio of energy flow distributed among channels is 77.2% for the left channel, 30.0% for the right channel, 22.2% for the upper channel, and 22.2% for the down channel.

From simulation results of Fig. 4, it is concluded that not all light propagates inside the channels. This is because the sum of the net energy flow ratio of the upper, right, and down channels is not the same as that of the left channel. This difference in the net energy flow is under 5% and also associated with the position of the single inserted rod. For light whose state is in the band gap of the bulk of PhC, it is safe to conclude that it could not pass through the bulk of PhC. It, however, must enter a small depth of the PhC when it propagates around the bulk of the PhC. In simulations, a small amount of light always propagates inside the PhC rather than inside the channels (Fig. 3). Because the detectors' length is $2a$, detectors only count the energy flow inside the channels. This means that the detectors do not count all the energy flow in the optical switch. A small amount of light detours the detectors without leaving any trace on the detectors.

The position-dependent net energy flow of the left channel is valley-shaped due to the various reflections in the left channel (Fig. 4). In our simulations, it is the net energy flow that is collected by the directional detectors. The left detector, whose direction is positive direction of the x-axis, counts the energy flow of the reflected wave as negative energy flow because the reflected wave passes through the left detector along the negative x-axis. The more powerful the reflected wave, the more negative energy flow the left detector collects. Assuming that the incident wave is same, the left detector consequently counts the less amount of net energy flow. The highest intensity of reflected wave in the left channel occurs when a single inserted rod is located at $(0,0)$. As a result, the minimum ratio of net energy flow of the left channel, 28.0%, corresponds to the location of the single inserted rod $(0,0)$. When the single

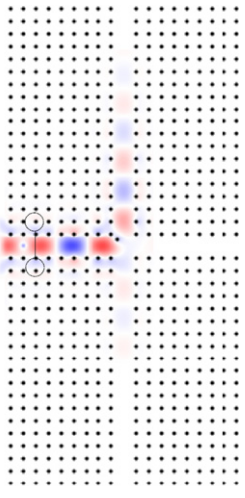

Fig. 3. Snapshot of E_z during the simulation (at time of $106a/c$) when the single rod is inserted at $(-0.5,-0.5)$. The red color represents positive E_z, the blue color negative E_z. The deep color means the larger magnitude of E_z, i.e. $|E_z|$. Some light detours (indicated by dotted circles) the detectors and could not be accumulated by the detectors. For interpretation of the references to color in this figure legend, the reader is referred to the web version of this article.

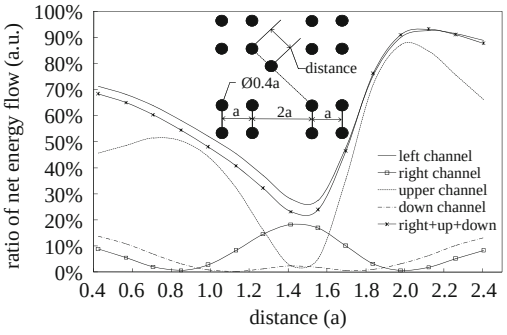

Fig. 4. Relation between the ratio of net energy flow in each channel and the position of single inserted rod. The curve labeled right+up+down represents the sum ratio of net energy flow in the right, upper, and down channels.

Please cite this article as: H.Z. Wang, et al., A 2D rods-in-air square-lattice photonic crystal optical switch, Opt. Int. J. Light Electron. Opt. (2010), doi:10.1016/j.ijleo.2009.06.002

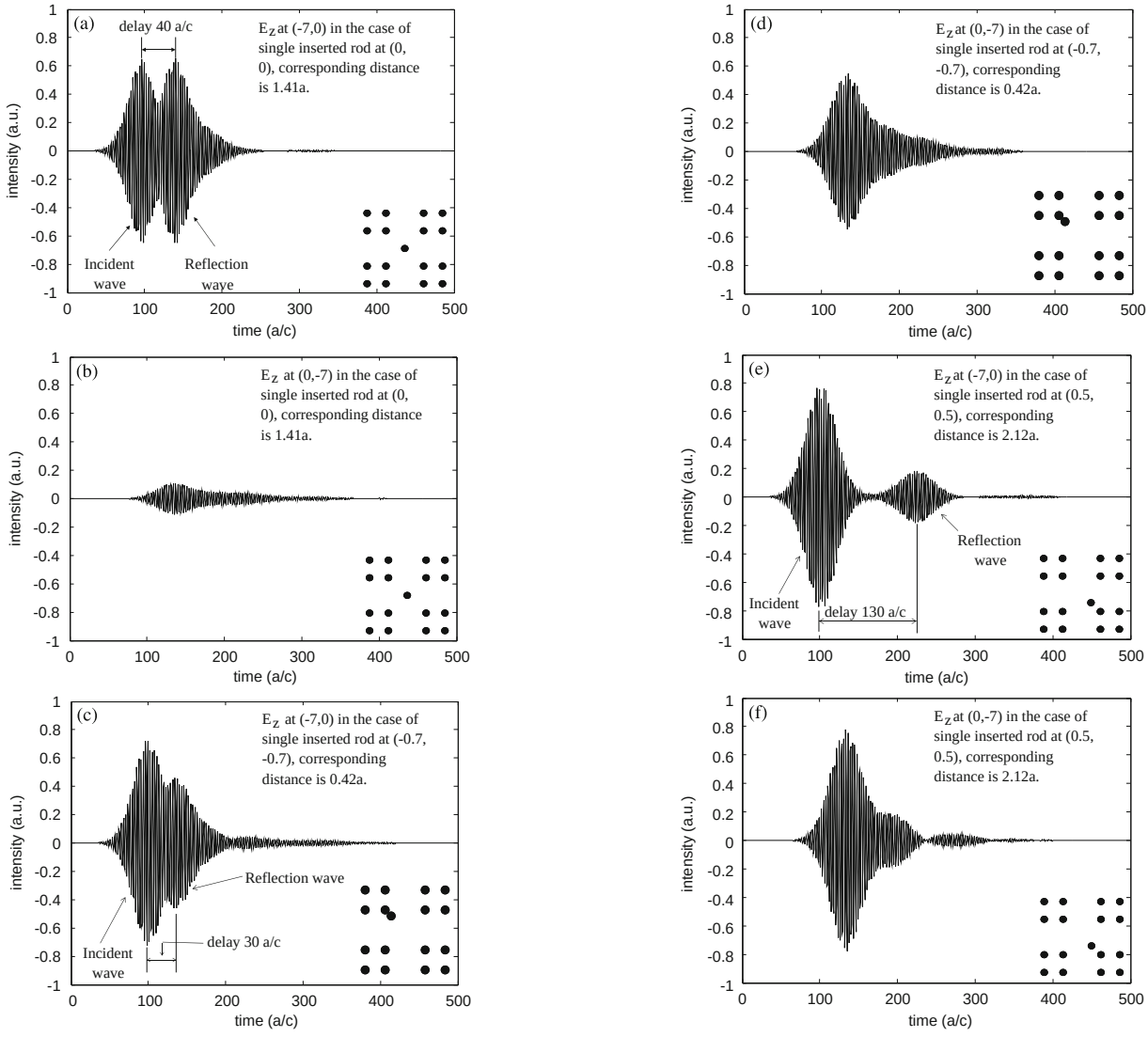

Fig. 5. Plot of E_z vs. time at the center of left detector $(-7,0)$ under the case of single inserted rod at (a) $(0,0)$, (c) $(-0.7,-0.7)$, and (e) $(0.5,0.5)$. Plot of E_z vs. time at the center of upper detector $(0,-7)$ under the case of single inserted rod at (b) $(0,0)$, (d) $(-0.7,-0.7)$, and (f) $(0.5,0.5)$. The corresponding distances are $1.41a$, $0.42a$, and $2.12a$, respectively.

Fig. 5. (*Continued*)

inserted rod is away from the location $(0,0)$, there is a weak reflected wave in the left channel. So, the left detector counts more net energy flow since a weak reflected wave has a less negative energy flow. This variable reflection of light is the reason for the valley shape of net energy flow ratio of the left channel. Obviously, this alterable reflection results from different positions of the single inserted rod.

The plots of E_z vs. time at point $(-7,0)$, which is the center of the left detector, are evidence that reflection wave exists. Fig. 5(a) corresponds to the case of distance of $1.41a$, in which the net energy flow of the reflected wave of 72.0% exists, based on the above analysis. In Fig. 5(a), the amplitude of the reflected wave is nearly the same as that of the incident wave. Both the incident wave and the reflected wave are clearly separated by a time delay of $40a/c$. In Fig. 5(c), the case for distance $0.42a$, the reflected wave is mixed together with the incident wave. According to the previous analysis of this case, the energy flow of the reflected wave is 28.7%, which is smaller than that of the case for distance $1.41a$. In the case of distance $0.42a$, the amplitude of the reflected wave is smaller than that of distance $1.41a$. In Fig. 5(c), both the incident and reflected waves are not clearly separated and the reflected wave delayed by $30\ a/c$ after the incident wave. Fig. 5(e) shows the case of distance $2.12a$, in which the energy flow of the reflected wave is 7.3% and smaller than those at distances $0.42a$ and $1.41a$, from the previous analysis. In Fig. 5(e), the amplitude of the reflected wave is the smallest among Fig. 5(a), (c), and (e). However, in the case of distance $2.12a$, the time delay between the incident and reflected waves, $130a/c$, is the largest among Fig. 5(a), (c), and (e). It can be concluded that the reflected wave was changed with respect to both amplitude and time delay in the case of variant position of a single inserted rod. As a result, the changed reflected wave affects the net energy flow ratio counted by the left detector. The more powerful the reflected wave, the less net energy flow counted by the left detector. It is noted that Fig. 5(a), (c), and (e) are plots at one point $(-7,0)$. However, the energy flow collected by the left detector is a line integral from $(-7,-1)$ to $(-7,1)$. E_z plots vs. time at one point in Fig. 5(a), (c), and (e) only provide a valuable and reasonable, but not strict, explanation to the valley-shaped net energy flow ratio of the left channel.

Assuming that the reflected wave is produced by a single inserted rod, whose position is $(0,0)$, the time delay between the incident and reflected waves at point $(-7,0)$ should be

Please cite this article as: H.Z. Wang, et al., A 2D rods-in-air square-lattice photonic crystal optical switch, Opt. Int. J. Light Electron. Opt. (2010), doi:10.1016/j.ijleo.2009.06.002

$(2[0-(-7)]a)/c=14a/c$ from the viewpoint of classic optics. However, the time delays in Fig. 5(a), (c), and (e) are much greater than $14a/c$. It shows that light does not propagate directly between the left detector and the single inserted rod. Light encountered more reflections with PhC walls of the left channel, which consequently increases the delay time of the reflection wave to a large extent.

Fig. 5(b), (d), and (f) show the plots of E_z vs. time at point $(0, -7)$, which is the center of the upper detector, corresponding to distances $1.41a$, $0.42a$, and $2.12a$, respectively. These plots illustrate there is one wave in the upper channel. The amplitude of E_z at the distance $2.12a$ [Fig. 5(f)] is larger than those at distances $1.41a$ [Fig. 5(b)] and $0.42a$ [Fig. 5(d)]. The greater amplitude of E_z, the more net energy collected by the upper detector. This conclusion is also illustrated in Fig. 4, in which the ratio of the net energy flow in the upper channel is 45.7% at a distance of $0.42a$, 2.5% at a distance of $1.41a$, and 84.9% at distance of $2.12a$. Even though the amplitude of E_z at $(0, -7)$ varies, its maximum amplitude roughly occurs at time 140 a/c, irrespective of the positions of the single inserted rod. Assuming that the incident energy flow passes the left detector at time 100 a/c [Fig. 5(a), (c), and (e)], the distributed wave arrives at the upper detector after 40 a/c.

The optical switch application may be considered as follows: when an appropriate Gaussian TM pulse enters this 2D optical rods-in-air square-lattice photonic crystal switch, 87.3% of incident energy enters the upper channel if the position of the single inserted rod is $(0.4, 0.4)$; if the single inserted rod shifts to position $(0.4, -0.4)$, the same amount of incident energy enters the down channel. This kind of switching function is popularly used in telecommunications.

Another possible application of this 2D rods-in-air square-lattice PhC structure is used as an optical intensity modulator. It is noticed [Fig. 4] that, when the position of single inserted rod is in the range $0.9a$–$1.4a$ and $1.5a$–$2.0a$, the ratio of net energy flow entering the upper channel is approximately linearly controlled by the position of the single inserted rod. In the distance range $0.9a$–$1.4a$, the ratio of modulation is from 5% to 50% of incident energy. In this distance range, the modulation coefficient is $(50–5\%)/(1.4a–0.9a)=90\%$ of the incident energy per distance unit (a). In the distance range $1.5a$–$2.0a$, the ratio of modulation is from 5% to 85% of incident energy. In this distance range, the modulation coefficient is $(85–5\%)/(2.0a–1.5a)=160\%$ of the incident energy per distance unit (a), larger than that in the range $0.9a$–$1.4a$. However, the ratio of net energy flow entering into the right channel increases greatly, up to 20%, in the distance range $1.0a$–$2.0a$. In other words, up to 20% of the incident energy is leaked into the right channel. This large leakage is a known issue of optical intensity modulator application.

In order to understand the influence of the size of the inserted rod to the energy flow, the inserted rod with various sizes from $0.3a$ to $0.5a$ was applied to the PhC. The simulation results show that the relationship between the ratio of net energy flow in each channel and the position of single inserted rod is as similar as that in the case of single inserted rod with diameter $0.4a$. It is found, by comparison, that the relationship between the ratio of net energy flow in each channel and the position of single inserted rod with various diameter ($0.3a$, $0.4a$, and $0.5a$) shift with the position of single inserted rod. The comprehensive discussion will be carried out in future publications.

It should be pointed out that this study was mainly focused on the energy flow inside a PhC; however, the special profile of the light affected by PhC and additional optical fibers at the entrance and exit of PhC have not been studied. New software is needed to investigate the special profile and interaction between PhC and external optical fibers.

4. Conclusions

A 2D rods-in-air square-rod photonic crystal optical switch was studied using simulation. It was found that the amount of energy entering different channels was strongly related with the position of a single inserted rod. Up to 87.3% of incident energy of TM Gaussian point source was switched into the upper channel. The relation between the position of the single inserted rod and net energy flow ratio in each channel has been discussed. The position of a single inserted rod affects the reflected wave of the left channel to a great extent. The time delay of the incident and reflected waves in the left channel is also largely related to the position of the single inserted rod. The magnitude of time delay shows that light experienced more reflections in the left channel. This investigation suggests that this compact 2D PhC optical switch structure could be a prospective and practical optical switching device, particularly in the field of integrating optical circuit.

Acknowledgements

This research was supported by the US Army Research Laboratory under Cooperative Agreement DAAD19-01-2-0014. The authors would like to thank Dr. Pedro Moss for his valuable suggestions and discussions.

References

[1] Eli Yablonovitch, Inhibited spontaneous emission in solid-state physics and electronics, Phys. Rev. Lett. 58 (20) (1987) 2059–2062.
[2] Sajeev John, Strong localization of photons in certain disordered dielectric superlattices, Phys. Rev. Lett. 58 (23) (1987) 2486–2489.
[3] Edilson A. Camargo, Harold M.H. Chong, Richard M. De La Rue, 2D Photonic crystal thermo-optic switch based on AlGaAs/GaAs epitaxial structure, Opt. Express. 12 (4) (2004) 588–592.
[4] Tao Chu, Hirohito Yamada, Satomi Ishida, Yasuhiko Arakawa, Thermooptic switch based on photonic-crystal line-defect waveguides, IEEE Photon. Technol. Lett. 17 (10) (2005) 2083–2085.
[5] Ahmed Sharkawy, Shouyuan Shi, Dennis W. Prather, Electro-optical switching using coupled photonic crystal waveguides, Opt. Express. 10 (20) (2002) 1048–1059.
[6] J. Danglot, O. Vanbésien, D. Lippens, A 4-port resonant switch patterned in a photonic crystal, IEEE Microwave Guided Wave Lett. 9 (7) (1999) 274–276.
[7] Ming-Chang M. Lee, Dooyoung Hah, Erwin K. Lau, Hiroshi Toshiyoshi, Ming Wu, MEMS-actuated photonic crystal switches, IEEE Photon. Technol. Lett. 18 (2) (2006) 358–360.
[8] Y. Kanamori, K. Inoue, K. Horie, K. Hane, Photonic crystal switch by inserting nano-crystal defects using MEMS actuator, in: Proceedings of the IEEE/LEOS International Conference on Optical MEMS 18–21 August 2003, Waikoloa, Hawaii, USA, pp. 107–108.
[9] K. Umemori, Y. Kanamori, K. Hane, A photonic crystal waveguide switch with a movable bridge slab, in: Proceedings of the IEEE/LEOS International Conference on Optical MEMS and Their Applications, 21–24 August 2006, Big Sky, Montana, USA, pp. 72–73.
[10] Ken-ichi Umemori, Yoshiaki Kanamori, Kazuhiro Hane, Photonic crystal waveguide switch with a microelectromechanical actuator, Appl. Phys. Lett. 89 (2) (2006) 021102.
[11] Amy E. Bieber, David F. Prelewitz, Thomas G. Brown, Richard C. Tiberio, Optical switching in a metal–semiconductor–metal waveguide structure, Appl. Phys. Lett. 66 (25) (1995) 3401–3403.
[12] Alain Haché, Martin Bourgeois, Ultrafast all-optical switching in a silicon-based photonic crystal, Appl. Phys. Lett. 77 (25) (2000) 4089–4091.
[13] Marin Soljačić, Mihai Ibanescu, Steven G. Johnson, Yoel Fink, J.D. Joannopoulos, Optimal bistable switching in nonlinear photonic crystals, Phys. Rev. E. 66 (5) (2002) 055601(R).
[14] Mehmet Fatih Yanik, Shanhui Fan, Marin Soljačić, High-contrast all-optical bistable switching in photonic crystal microcavities, Appl. Phys. Lett. 83 (14) (2003) 2739–2741.
[15] Takasumi Tanabe, Masaya Notomi, Satoshi Mitsugi, Akihiko Shinya, Eiichi Kuramochi, All-optical switches on a silicon chip realized using photonic crystal nanocavities, Appl. Phys. Lett. 87 (15) (2005) 151112(R).
[16] Takeshi Fujisawa, Masanori Koshiba, Finite_element modeling of nonlinear mach-zehnder interferometers based on photonic-crystal waveguides for all-optical signal processing, J. Lightwave. Technol. 24 (1) (2006) 617–623.
[17] Akio Higo, Satoshi Iwamoto, Masami Ishida, Yasuhiko Arakawa, Hiroyuki Fujita, Hiroshi Toshiyoshi, Design and fabrication on MEMS optical modulators integrated with Phc waveguide, in: Proceedings of the IEEE/LEOS

International Conference on Optical MEMS and their Applications, Finland, 1–4 August 2005, pp. 113–114.
[18] Steven G. Johnson, Christina Manolatou, Shanhui Fan, Pierre R. Villeneuve, J.D. Joannopoulos, H.A. Haus, Elimination of cross talk in waveguide intersections, Opt. Lett. 23 (23) (1998) 1855–1857.
[19] Mehmet Fatih Yanik, Shanhui Fan, Marin Soljačić, J.D. Joannopoulos, All-optical transistor action with bistable switching in a photonic crystal cross-waveguide geometry, Opt. Lett. 28 (24) (2003) 2506–2508.
[20] Cii-Chang Chen, Huang-Da Chien, Pi-Gang Luan, Photonic crystals beam splitters, Appl. Opt. 43 (33) (2004) 6187–6190.
[21] Young-Geun Roh, Sungjoon Yoon, Heonsu Jeon, Seung-Ho Han, Q-Han Park, Experimental verification of cross talk reduction in photonic crystal waveguide crossings, Appl. Phys. Lett. 85 (16) (2004) 3351–3353.
[22] Damian Goldring, Evgeny Alperovich, Uriel Levy, David Mendlovic, Analysis of waveguide-splitter-junction in high-index silicon-on-insulator waveguides, Opt. Express. 13 (8) (2005) 2931–2940.
[23] Selin H.G. Teo, A.Q. Liu, M.B. Yu, J. Singh, Fabrication and demonstration of square lattice two-dimensional rod-type photonic bandgap crystal optical intersections, Photon. Nanostruct. – Fundam. Appl. 4 (2006) 103–115.
[24] N. Moll, R. Harbers, R.F. Mahrt, G.-L. Bona, Integrated all-optical switch in a cross-waveguide geometry, Appl. Phys. Lett. 88 (2006) 171104.
[25] Pi-Gang, Kao-Der Chang, Periodic dielectric waveguide beam splitter based on co-directional coupling, Opt. Express. 15 (8) (2007) 4536–4545.
[26] Salim Boutami, et al., Photonic crystal-based MOEMS devices, IEEE J. Sel. Top. Quantum Electron. 13 (2007) 244–252.
[27] Steven G. Johnson, J.D. Joannopoulos, Block-iterative frequency-domain methods for Maxwell's equations in a planewave basis, Opt. Express. 8 (3) (2001) 173–190.
[28] Jean-Pierre Berenger, A perfectly matched layer for the absorption of electromagnetic waves, J, Comput. Phys. 114 (1994) 185–200.

Please cite this article as: H.Z. Wang, et al., A 2D rods-in-air square-lattice photonic crystal optical switch, Opt. Int. J. Light Electron. Opt. (2010), doi:10.1016/j.ijleo.2009.06.002